Original Article

CAMBRIDGE
UNIVERSITY PRESS

Abnormal dynamic functional network connectivity in unmedicated bipolar and major depressive disorders based on the triple-network model

Junjing Wang[1,2,*], Ying Wang[3*], Huiyuan Huang[2], Yanbin Jia[4], Senning Zheng[2], Shuming Zhong[4], Guanmao Chen[3], Li Huang[3] and Ruiwang Huang[2]

[1]Department of Applied Psychology, Guangdong University of Foreign Studies, Guangzhou 510006, China; [2]School of Psychology, Institute of Brain Research and Rehabilitation (IBRR), Center for the Study of Applied Psychology & MRI Center, Key Laboratory of Mental Health and Cognitive Science of Guangdong Province, South China Normal University, Guangzhou 510631, China; [3]Medical Imaging Center, First Affiliated Hospital of Jinan University, Guangzhou 510630, China and [4]Department of Psychiatry, First Affiliated Hospital of Jinan University, Guangzhou 510630, China

Abstract

Background. Previous studies have analyzed brain functional connectivity to reveal the neural physiopathology of bipolar disorder (BD) and major depressive disorder (MDD) based on the triple-network model [involving the salience network, default mode network (DMN), and central executive network (CEN)]. However, most studies assumed that the brain intrinsic fluctuations throughout the entire scan are static. Thus, we aimed to reveal the dynamic functional network connectivity (dFNC) in the triple networks of BD and MDD.
Methods. We collected resting state fMRI data from 51 unmedicated depressed BD II patients, 51 unmedicated depressed MDD patients, and 52 healthy controls. We analyzed the dFNC by using an independent component analysis, sliding window correlation and k-means clustering, and used the parameters of dFNC state properties and dFNC variability for group comparisons.
Results. The dFNC within the triple networks could be clustered into four configuration states, three of them showing dense connections (States 1, 2, and 4) and the other one showing sparse connections (State 3). Both BD and MDD patients spent more time in State 3 and showed decreased dFNC variability between posterior DMN and right CEN (rCEN) compared with controls. The MDD patients showed specific decreased dFNC variability between anterior DMN and rCEN compared with controls.
Conclusions. This study revealed more common but less specific dFNC alterations within the triple networks in unmedicated depressed BD II and MDD patients, which indicated their decreased information processing and communication ability and may help us to understand their abnormal affective and cognitive functions clinically.

Introduction

The bipolar disorder (BD) and major depressive disorder (MDD) are two severe affective disorders in our society with high suicide rates and a heavy social burden (Fountoulakis, 2010). Clinically, BD shows recurring episodes of hypomania/mania and depression, while MDD only shows depressive episodes. For their common depressive episodes and the higher prevalence of depression relative to specific mania symptoms in BD, it is necessary to highlight the neural physiopathology of BD and MDD during depressive episodes and then to detect their common and specific neural physiopathology.

Based on resting state fMRI (RS-fMRI) data and functional connectivity (FC) analysis, the triple-network model has been widely used to indicate the neural physiopathology of various diseases. The triple-network model, which was proposed by Menon (2011), is a unifying model to explain the neural physiopathology of psychiatric and neurological disorders given the fact that the dysfunctions of these disorders occur at a network level rather than in an individual brain area. This model examines 'core' brain networks supporting cognitive, perceptual, affective, and social functions, involving the salience network (SN), default mode network (DMN) and central executive network (CEN), which are thought to be abnormally organized in many psychiatric disorders (Menon, 2011). Up to date, the altered FC properties within the triple networks have been revealed in BD and MDD patients. In depressed BD patients, Gong *et al.* (2019) detected disrupted FC within the DMN and SN compared with controls. For depressed MDD patients, several studies (de Kwaasteniet *et al.*, 2014; Wei *et al.*, 2015; Gong *et al.*, 2017; Jiang *et al.*, 2017) have revealed altered FC within the SN, DMN, CEN, as well

as between the DMN and SN, between the SN and CEN, and between the CEN and DMN compared with controls. For depressed and remitted MDD patients, Dong et al. (2018) found that both had decreased FC within the CEN, increased FC between the SN and CEN, and decreased FC between the DMN and CEN compared with controls, suggesting the state-independent FC alterations within the triple networks in MDD patients. Further, by including both depressed BD and MDD patients, Goya-Maldonado et al. (2016) compared FC in core regions of the fronto-parietal network (including the core regions of CEN), cingulo-opercular networks (including the core regions of SN), and DMN. They found increased FC in the fronto-parietal network in depressed BD patients and increased FC in the DMN in depressed MDD patients compared with controls. Similarly, one of our studies (Wang et al., 2018) compared FC alterations in the triple networks of depressed BD and MDD patients compared with controls. We found FC alterations within the DMN and SN as well as between the DMN and CEN in both BD and MDD patients, but specific FC alterations between the CEN and SN in BD patients. Taken together, the abnormal FC properties within the triple networks existed in BD and MDD; these abnormalities seem to be state-independent, and there are some common and specific abnormalities between BD and MDD. However, these studies above all regarded the functional properties of the entire RS-fMRI scan as static but not dynamic.

In fact, human brain is never in static state and a growing number of studies have indicated that the FC shows noticeable variations at rest in the absence of any external stimuli (Tagliazucchi and Laufs, 2014; Barttfeld et al., 2015; Gonzalez-Castillo et al., 2015; Karahanoglu and Van De Ville, 2015). This dynamic FC (dFC) exhibits highly structured spatiotemporal patterns in which a set of metastable FC patterns, known as dFC states, reliably recur across time and subjects. A number of studies have focused on dFC states and found that they may be associated with ongoing human cognition (Gonzalez-Castillo et al., 2015), consciousness level (Barttfeld et al., 2015), flexible behavior (Shanahan, 2010; Tognoli and Kelso, 2014), brain development (Hutchison and Morton, 2015), and neuropsychiatric disorders (Zhao et al., 2017; Negwer et al., 2018). Specifically, in remitted BD patients, Nguyen et al. (2017) studied dFC within the DMN and found decreased dFC between the medial prefrontal cortex (mPFC) and posterior cingulate cortex (PCC). In addition, Rashid et al. (2014) compared dFC properties between schizophrenia, mixed psychotic and non-psychotic BD patients, and controls, and identified different patterns of connectivity involving the frontal and frontal–parietal regions between schizophrenia and BD patients. They also found that the dFC was more informative than stationary FC in classifying the BD patients from schizophrenia patients (Rashid et al., 2016). In depressed MDD patients, previous studies revealed abnormal dFC variability between the mPFC and insular regions (Kaiser et al., 2016), between the mPFC and PCC (Wise et al., 2017), and between the DMN and CEN (Demirtas et al., 2016). Further, by including both depressed BD and MDD patients, Pang et al. (2018) detected common and specific alterations in dFC related to the insular cortex. Altogether, these studies revealed that both BD and MDD had dFC abnormalities; the abnormalities always involve in the SN, DMN, and CEN from the perspective of network, and there are some common and specific abnormalities between BD and MDD. However, up to date, few studies have analyzed the dynamic functional network connectivity (dFNC) between networks composing the triple networks of BD and MDD.

In this study, by combining RS-fMRI data with the triple-network model, we aimed to reveal the dFNC alterations between the SN, DMN, and CEN in unmedicated BD and MDD patients during depressive episodes. In order to reduce the confounding factors, such as the subtype-, medicine-, and states-related effects, we only included the unmedicated BD-II (refer to BD in the following) and MDD patients during depressive episodes, matching their number of episodes, age of onset, duration of illness and clinical states. Based on the findings mentioned above and our previous studies on depressed BD and MDD patients (Niu et al., 2017; Wang et al., 2017b, 2017c; Chen et al., 2018; He et al., 2018; Wang et al., 2018), we made the following hypotheses: (1) the BD and MDD patients have dFNC alterations within the triple networks; (2) there are more common and less specific alterations between the BD and MDD patients.

Materials and methods

Subjects

A total of 51 currently depressed adults diagnosed with BD II (24M/27F, age = 26.35 ± 8.79 years old) and 51 currently depressed adults diagnosed with MDD (22M/29F, age = 28.45 ± 8.47 years old) were recruited from the Psychiatry Department of the First Affiliated Hospital of Jinan University, Guangzhou, China. The diagnoses of BD and MDD were based on the Structured Clinical Interview for DSM-IV. The clinical state of each patient was assessed using the 24-item Hamilton Depression Rating Scale (HAMD) (Meda et al., 2014) and the Young Mania Rating Scale (YMRS) (Young et al., 1978) during the 7-day period prior to the scan. The inclusion criteria were a HAMD-24 total score >21 for the MDD patients and a YMRS total score <7 combined to a HAMD-24 total score >21 for the BD patients (Wang et al., 2015). The exclusion criteria were patients with other Axis-I psychiatric disorders (except for MDD, BD, and anxiety disorders), Axis-II psychiatric disorders, a history of organic brain disorder, neurological disorders, mental retardation, cardiovascular diseases, alcohol or substance abuse, pregnancy, or any physical illness. At the time of scanning, all patients were either medication-naive or had been unmedicated for at least 5 months. None of the patients had received psychotherapy or electroconvulsive therapy prior to participating in the current study.

In addition, we recruited 52 gender-, age-, and education-matched healthy subjects (20M/32F, age = 29.71 ± 11.19 years old) as controls via local advertisements. They were carefully screened through a diagnostic interview, the Structured Clinical Interview for DSM-IV (non-patient edition), to rule out the presence of current or past psychiatric illness. Further exclusion criteria for the controls were any history of psychiatric illness in first-degree relatives and any current or past significant medical illness or mental disorders.

All subjects were right-handed according to their self-report. The study was approved by the Ethics Committee of the First Affiliated Hospital of Jinan University, Guangzhou, China. The procedures were carried out in accordance with the approved guidelines. All subjects signed a written informed consent form after a full written and verbal explanation of the study. Two experienced clinical psychiatrists (Y.J. and S.Z.) confirmed that all subjects had the ability to consent to participate in the examination independently.

Data acquisition

All MRI data were obtained on a 3 T GE MR750 scanner with an eight-channel phased-array head coil in the Medical Center of the

First Affiliated Hospital of Jinan University, Guangzhou. The RS-fMRI datasets were acquired using a single-shot gradient-echo EPI sequence with the following parameters, repetition time (TR) = 2000 ms, echo time (TE) = 25 ms, flip angle (FA) = 90°, field of view (FOV) = 240 mm × 240 mm, data matrix = 64 × 64, thickness/gap = 3.0/1.0 mm, 35 axial slices covering the whole-brain, and 210 volumes acquired in about 7 min. During the RS-fMRI scan, each subject was requested to keep their eyes closed but not to fall asleep, and to relax the mind but not to think about anything in particular. In addition, the routine axial T1-weighted fluid attenuation inversion recovery and fast spin-echo T2-weighted MR sequences were also applied to obtain brain images to confirm the absence of brain structural and signal abnormality.

Data preprocessing

The RS-fMRI data were preprocessed using SPM 12 (https://www.fil.ion.ucl.ac.uk/spm/software/spm12/) and DPARSF Advanced Edition (http://restfmri.net/forum/DPARSF). For each subject, the first 10 volumes of the RS-fMRI dataset were discarded to allow for MR signal equilibrium, leaving 200 volumes for further analyses. The remaining functional images were first corrected for the acquisition time delay between slices within the same TR, and then were realigned to the first volume for correcting the inter-TR head motion. This realignment calculation provided a record of head motion within the RS-fMRI scan. All of the subjects in this study satisfied our criteria for head motion with displacement <1.5 mm in any plane and rotation <1.5° in any direction. The corrected RS-fMRI data were spatially normalized to the Montreal Neurological Institute (MNI) space and were resampled to a voxel size of 3 mm × 3 mm × 3 mm. Then the normalized images were spatially smoothed using an isotropic Gaussian kernel of 6 mm full-width-at-half-maximum.

After preprocessing, we further processed the residual RS-fMRI data (the preprocessed data) according to the following steps illustrated in Fig. 1.

Group independent component analysis and post-processing

The preprocessed fMRI data were decomposed into different functional networks using a group-level spatial independent component analysis (ICA) in GIFT package (version 3.0a) (Calhoun *et al.*, 2001; Calhoun, 2004). First, the data reduction was conducted to decrease computational complexity using a two-stage principal component analysis. Precisely, the preprocessed fMRI data for each subject were first dimension-reduced temporally and then the reduced data from all subjects were concatenated into a single dataset, or the grouped data, along the temporal dimension and passed through another dimension reduction. Second, ICA was performed to decompose the grouped data into automatically estimated 29 independent components (ICs) using an Infomax algorithm (Bell and Sejnowski, 1995). In this step, the spatial map and the time course of BOLD signal were generated for each IC. This step was repeated 100 times using the ICASSO algorithm for assessing the repeatability or stability of ICs (Himberg *et al.*, 2004). Finally, the ICs for each subject were derived from a group ICA back reconstruction step and were converted into z-scores (Calhoun *et al.*, 2001). This provided subject-specific spatial maps and time courses which were further used to make group-level random-effects inferences (one sample t test). Thus, a group level t-map was generated for each IC and this t-map was used to identify the brain regions involved in the corresponding IC.

Then we identified ICs of interest by using the automatic identification method and the visual screening based on previous reported spatial maps. The detailed descriptions were displayed in online Supplementary materials. At last, we determined the five ICs, which correspond to the anterior DMN (aDMN), posterior DMN (pDMN), left CEN (lCEN), right CEN (rCEN), and SN.

In addition, we applied post-processing steps, including linear, quadratic, and cubic detrending, regression of their temporal derivative, removal of detected outliers, and low-pass filtering with a high-frequency cutoff of 0.1 Hz, to the IC time course to remove trends associated with scanner drift and movement-related artifacts. We have detected the outliers based on the median absolute deviation, as implemented in 3D DESPIKE. Outliers were replaced with the best estimate using a third-order spline fit to the clean portion of the time courses. At last, we used the residual time courses to do the following dFNC analyses.

dFNC estimation

We computed Pearson's correlations between time courses of ICs using the sliding window approach, creating tapered windows by convolving a rectangle (length = 22 TRs) with a Gaussian of σ = 3 TRs. The onset of each window progressively slid in steps of one TR from that of the previous one, resulting in 178 windows. The window length of 22 TRs was chosen because previous studies (Allen *et al.*, 2014; Leonardi and Van De Ville, 2015) have shown that a window length of 22 TRs may provide a good trade-off between the quality of the FNC estimate and the temporal resolution. To characterize the full covariance matrix, we estimated covariance from the regularized precision matrix or the inverse covariance matrix (McGuffin *et al.*, 2003). Following the graphical LASSO method of Friedman (Vandeleur *et al.*, 2014), we placed a penalty on L1-norm of the precision matrix to promote sparsity. The regularization parameter λ was optimized separately for each subject by evaluating the log-likelihood of unseen data (windowed covariance matrices from the same subject) in a cross-validation framework. Then the 5 × 5 dFNC windows were concatenated to form a 5 × 5 × 178 array which was used to represent the temporal changes of inter-network covariance (correlation) as a function of time for each subject.

dFNC variability

The temporal variability in dFNC was estimated using the standard deviation of inter-network correlation across sliding windows. Larger standard deviations indicate more variable (or less stable) FNC between networks.

dFNC states

For all the windowed 5 × 5 FNC matrices, we applied the k-means algorithm to divide the dFNC windows into separate clusters. First, we estimated the variability of inter-network correlation across sliding windows and selected the windows with local maxima in the FC variance as subject exemplars. Then, we performed a k-means analysis on the set of all the subject exemplars with a random initialization of the centroid positions. $k = 4$ was determined using the elbow criterion (Allen *et al.*, 2014). We repeated the clustering algorithm 500 times to increase the chance of escaping the local minima. The correlation distance function was chosen because it is more sensitive to the dFNC pattern, regardless of magnitude (Allen *et al.*, 2014). These resulting
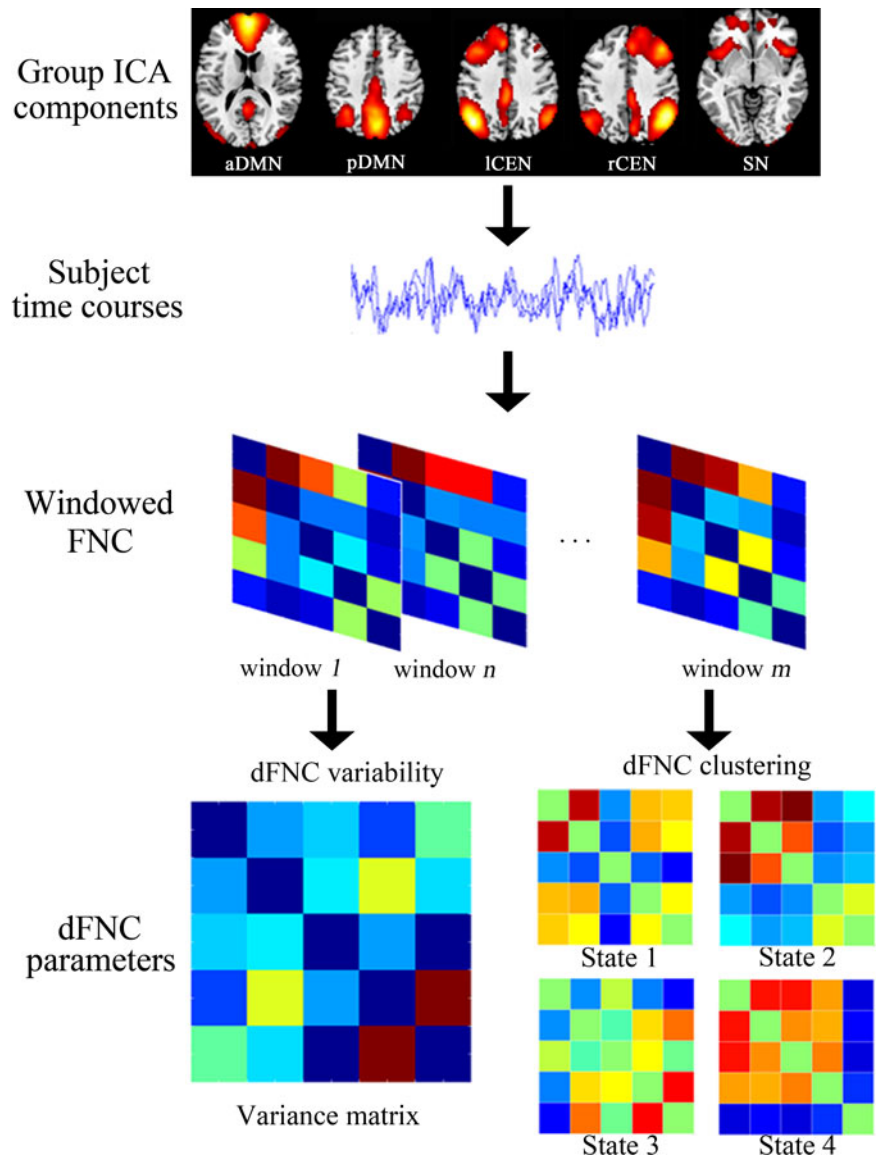
Fig. 1. Flowchart for the dynamic functional network connectivity (dFNC) analysis in this study. For the RS-fMRI data of all subjects, we first used group independent component analysis (groupICA) to parcellate the data into 29 independent components (ICs), and then selected the ICs corresponding to the networks of aDMN, pDMN, lCEN, rCEN, and SN. Then we adopted the sliding window approach to analyze the dFNC for the obtained 178 time windows. In each of the time windows, the inter-network FNC or Pearson's correlation was calculated between the time courses for each pair of networks. Afterwards, we calculated the dFNC variability across windows, clustered the time windows for all the participants using the k-means algorithm, and estimated the dFNC properties. aDMN, anterior default mode network; pDMN, posterior default mode network; lCEN, left central executive network; rCEN, right central executive network; SN, salience network.

centroids were then used as starting points to cluster the dFNC windows for all the subjects.

Finally, all time windows of all subjects were clustered into four states, State 1, State 2, State 3, and State 4. Then we calculated the dFNC properties, including the reoccurrence fraction and dwell time in each state as well as the transition number between different states for each subject. The reoccurrence fraction is the proportion of time spent in each state as measured by percentage. The mean dwell time represents how long the participant stayed in a certain state, which was calculated by averaging the number of consecutive windows belonging to one state before changing to other states. The transition number represents how many times either state changed from one to another, counting the number of times a switch occurred, with more transitions representing less stability over time.

Statistical analysis

Group comparison

Considering that the data distribution may bias the statistical results in parametric tests, we used the non-parametric tests in our statistics ($p < 0.05$). A permutation one-way analysis of variance (ANOVA) was used to detect differences in age and education level between the BD, MDD, and control groups. A Pearson's χ^2-test was used to detect difference in gender between the BD, MDD, and control groups. For clinical variables, a permutation two-sample t test was used to detect differences in the number of episodes, age of onset, duration of illness, HDRS24, and YMRS scores between the BD and MDD groups.

In addition, a permutation one-way analysis of covariance (ANCOVA) was conducted to detect the group effect on the dFNC parameters, including the dFNC variability, reoccurrence fraction and dwell time for each dFNC state, and transition number between states ($p < 0.05$). In the calculations, we took age, gender, and years of education as covariates. A post-hoc analysis was also carried out for the dFNC parameters that showed group effects.

Brain-behavioral relationship

For each of the dFNC parameters showing significant group effects (one-way ANCOVA, $p < 0.05$), we estimated Pearson's

Table 1. Demographics and clinical characteristics of the BD patients, MDD patients, and healthy controls in this study

Parameters	BD ($n = 51$)	MDD ($n = 51$)	Controls ($n = 52$)	p-value
Age (years old)	26.35 ± 8.79	28.45 ± 8.47	29.71 ± 11.19	0.20[a]
Gender (female/male)	27/24	29/22	32/20	0.68[b]
Education (years)	13.98 ± 2.60	13.22 ± 2.89	14.23 ± 2.82	0.10[a]
Number of episodes	2.22 ± 1.89	2.00 ± 1.82	NA	0.26[c]
Age of onset (years)	23.24 ± 8.56	25.31 ± 9.09	NA	0.12[c]
Duration of illness (months)	29.08 ± 37.07	32.29 ± 3.51	NA	0.35[c]
HAMD	25.80 ± 5.35	25.20 ± 5.81	2.88 ± 1.80	0.00[a]
YMRS	2.80 ± 3.67	2.92 ± 3.63	0.47 ± 0.90	0.00[a]

BD (MDD), bipolar (major depressive) disorder; HAMD, Hamilton Depression Rating Scale; YRMS, Young Mania Rating Scale.
[a]The p-value was obtained from permutation ANOVA.
[b]The p-value was estimated from Pearson's χ^2-test
[c]The p-value was calculated from permutation two-sample t test
NA, not applicable

correlation between the parameter and each of the clinical variables in the BD and MDD groups, separately ($p < 0.05$). The clinical variables included the HAMD score, number of episodes, onset age of illness, and total duration of illness. In this analysis, we also took the age, gender, and years of education as covariates.

Results

Demographic information

Table 1 lists the demographic and clinical characteristics of the BD, MDD patients, and controls. No significant difference was detected in age, gender, and education level between the three groups. Additionally, no significant difference was found in depression severity, illness duration, and onset age of illness between the BD and MDD groups.

ICs of interest

The five ICs of interest, aDMN, pDMN, lCEN, rCEN, and SN, which were selected from the 29 ICs (one sample t test, $p < 0.001$, FDR corrected) were shown in online Fig. S1 in Supplementary materials. The spatial layout of each IC was consistent with previous studies (Beckmann et al., 2005, Damoiseaux et al., 2006, Smith et al., 2009).

dFNC variability

Figure 2a shows the mean dFNC variability across windows in the BD, MDD patients, and controls, respectively. Figure 2b shows the dFNC variability with significant group effect (one-way ANCOVA, $p < 0.05$) and the corresponding box plots for post-hoc analyses. Briefly, both the BD and MDD patients had decreased dFNC variability between pDMN and rCEN compared with the controls. The MDD patients had specific decreased dFNC variability between aDMN and rCEN compared with the BD patients and controls.

dFNC states and properties

Figure 3 shows the four identified states with highly structured FC that recurred throughout individual scans and across subjects, as well as their occurrence time and percentage. In State 1, the DMN had negative FNC with lCEN but positive FNC with rCEN. The SN had positive FNC with DMN and rCEN but negative FNC with lCEN. In State 2, the DMN had positive FNC with lCEN but negative FNC with rCEN. The SN had negative FNC with DMN and lCEN but positive FNC with rCEN. In State 3, the FNC within the triple networks was very sparse. In State 4, the DMN had positive FNC with CEN, and the SN had negative FNC with both DMN and CEN. Moreover, we found positive connections between aDMN and pDMN in states with dense connections (States 1, 2, and 4).

For dFNC properties (one-way ANCOVA, $p < 0.05$), we found significant increased reoccurrence fraction (Fig. 4a) and dwell time (Fig. 4b) in State 3 in both the BD and MDD patients compared with the controls. However, no significant group effect was found in transition number.

Discussion

The present study analyzed the dFNC in the triple networks of depressed BD and MDD patients and highlighted the temporal properties of dFNC states and the dFNC variability. The main findings were as follows: (1) the dFNC within the triple networks could be clustered into four configuration states, three of them showing dense connections (States 1, 2, and 4) and one of them showing sparse connections (State 3); (2) the analyses in temporal properties of dFNC states showed that both the BD and MDD patients spent more time in State 3 with significant increased reoccurrence fraction and dwell time compared with the controls; (3) the analysis of dFNC variability showed that both the BD and MDD patients had decreased dFNC variability between pDMN and rCEN compared with the controls, while the MDD patients had specific decreased dFNC variability between aDMN and rCEN compared with either the BD patients or controls. These results validated previous demonstrations of abnormal FC within the triple networks (Menon, 2011; Wei et al., 2015; Zheng et al., 2015; Goya-Maldonado et al., 2016) and abnormal dFC properties (Demirtas et al., 2016; Kaiser et al., 2016; Wise et al., 2017) in BD and MDD patients. Our findings further highlighted the more common and less specific dFNC alterations in the triple networks of BD and MDD patients, and suggested that the dFNC in the triple networks of BD and MDD is characterized by more frequent state of sparse connections and decreased dynamic variability.

Fig. 2. The mean functional network connectivity (dFNC) variability across the time windows in the BD, MDD, and control groups. (*a*) For each subject group; (*b*) Group effect. The symbol of '+' indicates the inter-network dFNC variability showing significant group effect ($p < 0.05$, one-way ANCOVA). The post-hoc analysis was performed for the dFNC variability showing significant group effect. Symbols of ◊, Δ, and ○ in the scatter plot indicate the value of dFNC variability for a subject in the BD, MDD, and control groups, respectively. Red dots indicate outliers. The box plot shows the median (red line), interquartile range (blue lines), and sample minimum and maximum values (dark lines). The horizontal lines on top indicate pairwise comparisons that survived statistical thresholds: **$p < 0.01$; *$p < 0.05$. BD (MDD), bipolar (major depressive) disorder; aDMN, anterior default mode network; pDMN, posterior default mode network; lCEN, left central executive network; rCEN, right central executive network; SN, salience network; NA, not applicable.
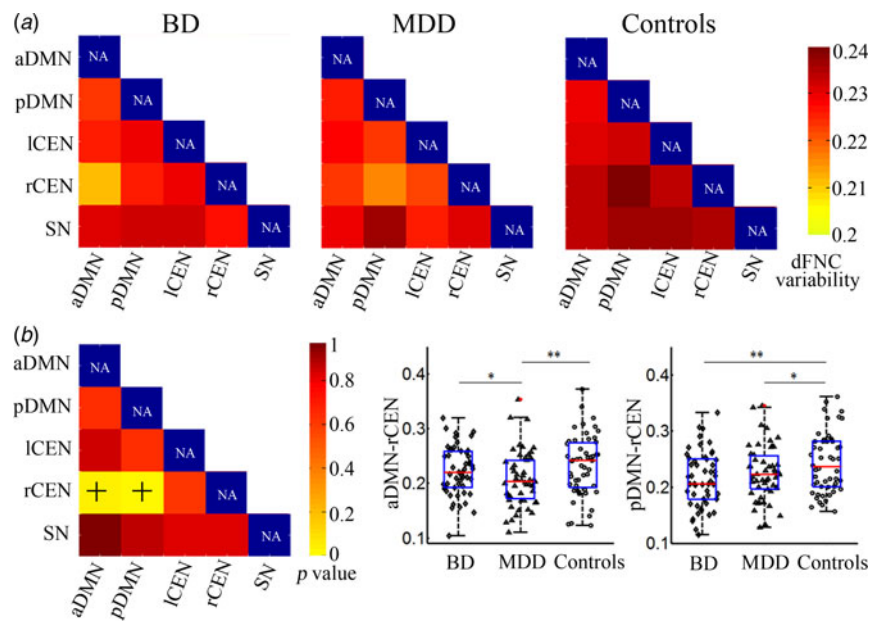

Fig. 3. The centroid of each functional network connectivity state, and the total number and percentage of occurrence of each connectivity state. aDMN, anterior default mode network; pDMN, posterior default mode network; lCEN, left central executive network; rCEN, right central executive network; SN, salience network.
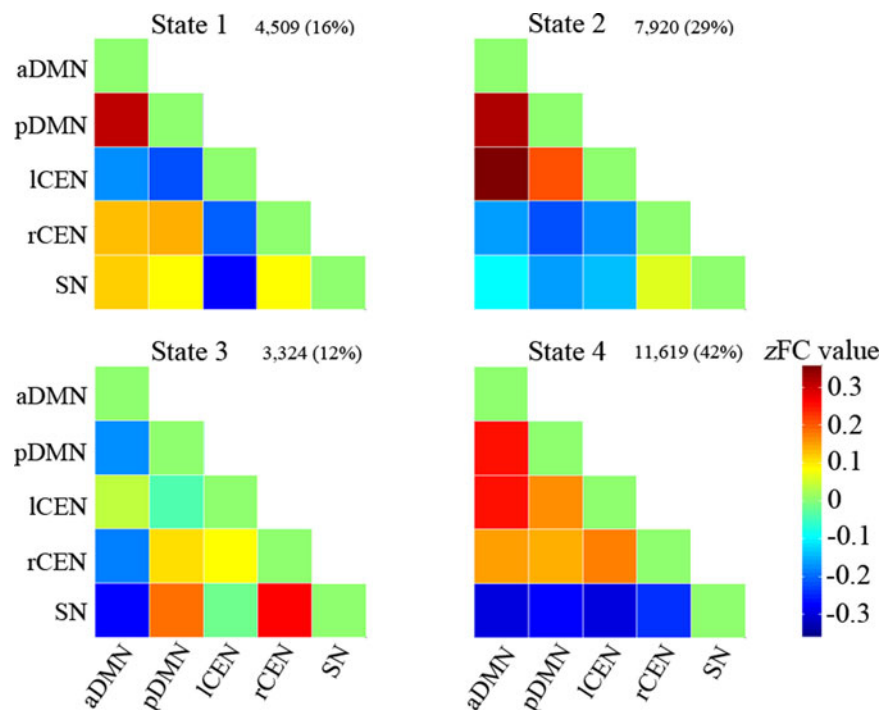
The four FNC configuration states detected in the present study provided dynamic interactive relationship within the triple networks. Previous studies (Fox *et al.*, 2005; Fransson, 2005; Sridharan *et al.*, 2008; Murphy *et al.*, 2009; Chen *et al.*, 2013; Goulden *et al.*, 2014) have used various measures to investigate the functional relationship between the SN, DMN, and CEN, and indicated that the SN drives the switching between DMN and CEN, and the CEN and SN negatively regulated the DMN. However, several previous studies reported inconsistent FNC patterns within the triple networks (Manoliu *et al.*, 2013; Manoliu *et al.*, 2014a; Abbott *et al.*, 2016; Wang *et al.*, 2017a) when taking the entire RS-fMRI scan as a static duration. For example, Abbott

et al. (2016) found that the DMN was negatively connected with both the FPN and SN, and the FPN was positively connected with the SN. Wang *et al.* (2017a) found that the SN was negatively connected with the pDMN while the other FNC within the triple networks were positive. Manoliu *et al.* (2013, 2014b) found that the SN was negatively correlated with the ventral CEN and inferior pDMN, the dorsal CEN was negatively correlated with the aDMN and inferior pDMN, and the other FNC within the triple networks were positive. These FNC patterns above were inconsistent with our detected four FNC states, either. A possible reason for this inconsistency may be that the FNC pattern within the triple networks during the entire RS-fMRI scan period is not static but dynamic,
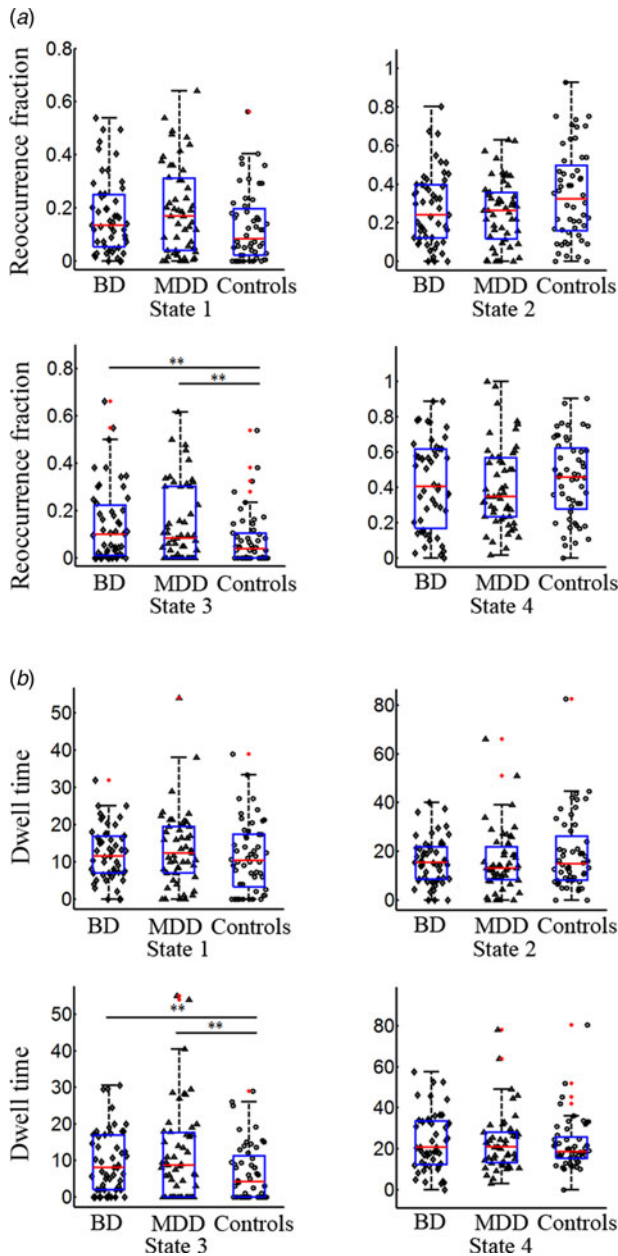
Fig. 4. Comparison of group effect of the functional network connectivity (dFNC) properties in each dFNC state between the BD, MDD, and control groups ($p < 0.05$, one-way ANCOVA). (a) Reoccurrence fraction, and (b) dwell time. The post-hoc analysis was performed for the dFNC properties showing significant group effect. Symbols of ◇, Δ, and ○ in the scatter plot indicate the dFNC properties for a subject in the BD, MDD, and control groups, respectively. Red dots indicate outliers. The box plot shows the median (red line), interquartile range (blue lines), and sample minimum and maximum values (dark lines). The horizontal lines on top indicate pairwise comparisons that survived statistical thresholds: **$p < 0.01$; *$p < 0.05$. BD (MDD), bipolar (major depressive) disorder.

different sparse and dense connected states and emphasized the roles of dFNC states and dFNC variability, which is consistent with our study. In total, the four FNC configuration states detected in the present study could provide more information about the dynamic interactive relationships within the triple networks in adults than only focusing on one static FNC pattern.

Further, both the BD and MDD patients spent more time in State 3 with sparse connections compared with the controls, including the increased reoccurrence fraction and dwell time (Fig. 4). Correlation analysis revealed that the reoccurrence fraction of State 3 was significantly positively correlated with the illness duration in the BD patients (online Fig. S2 in Supplementary materials). This indicated that as the disease accumulates, the BD patients spent more time in State 3. In State 3, the FNC within and between the triple networks are much lower than in other states (Fig. 3). The fact that patients spent longer time in the state with sparse connections is indicative of decreased information communication within the triple networks. The finding may help to explain the previous reported conclusions of decreased information communication ability in depressed (Meng et al., 2014; Wang et al., 2017c) and remitted MDD (Bai et al., 2012; Li et al., 2017), as well as depressed (Wang et al., 2017c) and remitted BD (Leow et al., 2013). For the existed decreased information communication ability across states, we may infer that the decreased information communication is state-independent in BD and MDD patients. In addition, considering that the interactions within the triple networks are responsible for maintaining information processing, such as cognitive, perceptual, affective, and social functions (Menon, 2011), we deduced that the increased time in sparse connections within the triple networks may account for the clinical symptoms of abnormal affective and cognitive processing and communication in depressed BD and MDD patients (Diener et al., 2012).

We also found decreased dFNC variability in the depressed patients compared with the controls, such as the decreased dFNC variability between pDMN and rCEN common to both the BD and MDD patients, and the decreased dFNC variability between aDMN and rCEN specific to the MDD patients (Fig. 2). A higher brain variability may reflect a greater complexity and greater capacity for information processing (Marusak et al., 2017). Thus, the decreased dFNC variability in our study may indicate decreased ability for information processing in depressed BD and MDD patients. The DMN and CEN can co-active with each other to perform particular mental tasks (Angst et al., 2010). The abnormal stationary FC between DMN and CEN has been reported in BD and MDD patients in depressive state (Sheline et al., 2010; Ye et al., 2012; de Almeida and Phillips, 2013; Manoliu et al., 2014a; Dong et al., 2018) and remitted state (Dong et al., 2018). Thus, the decreased dFNC variability between DMN and CEN may indicate a state-independent impairment in information processing in BD and MDD patients.

In addition, the dFNC variability between rCEN and aDMN or between rCEN and pDMN has different roles in specific and common alterations of BD and MDD patients, which remind us of the different roles of aDMN and pDMN in the physiopathology of depression. The aDMN mainly includes the mPFC, which is believed to be associated with social cognition involving the monitoring of one's own psychological states, and mentalizing about the psychological states of others (Broyd et al., 2009; Kaiser et al., 2016). The pDMN mainly includes the PCC or precuneus, which is supposed involving the continuous sampling of external and internal environments (Raichle et al., 2001), and may play a role

resulting in various FNC patterns in different scan periods. Considering that the brain activity during RS-fMRI scan is dynamic, Marusak et al. (2017) analyzed the dFNC within the triple networks in children and revealed six different states. We cannot directly compare the four states obtained in the present study with their six states, because they recruited children but not adults and they divided each network into several subnetworks and focused on the FNC between subnetworks. But they also detected

in processing of emotionally salient stimuli related to episodic memory (Maddock, 1999). In addition, the CEN is responsible for high-level cognitive functions, such as planning, decision making, attention, and working memory (Menon, 2011). Thus, the specific decreased dFNC variability between aDMN and rCEN in the MDD patients may give us indications about their seriously imbalanced monitoring of own and others' states, which may help us to understand their abnormal self-referential processing during their unique characterized episode of depression clinically. While the common decreased dFNC variability between pDMN and rCEN indicated their imbalanced sampling between external and internal stimuli, especially in affective stimuli, which may help us to understand their common affective dysfunction clinically.

Limitations

This study has several limitations. First, we cannot predict whether some MDD patients will later switch to BD patients in the absence of longitudinal data. However, we tried our best to reduce the possibility of misdiagnosis. Two experienced, senior psychiatrists carried out the diagnosis. We also tracked the MDD patients after we acquired the data and found that none of the patients had switched to another diagnosis type by the time of the submission of this manuscript. Second, considering that our study is an exploratory one, our results should be interpreted cautiously since the results cannot survive multiple comparison corrections. Third, our results are specific to the depressive episodes of BD and MDD patients. A longitudinal study is needed to test whether the findings are state-dependent or trait-dependent in the future. Thus, we can compare the differences between state and trait in terms of dFNC in the triple networks. Fourth, we only included BD II type in the present study, which may limit the generalizability of our findings to other BD types. Fifth, we did not collect any questionnaires for supplementary analysis in our study and, in future studies, we would better add this.

Conclusion

In summary, our study detected common and specific dFNC abnormalities in the triple networks of unmedicated depressed BD II and MDD patients. On one side, we detected the common alterations of more frequent state of sparse connections and decreased dFNC variability between pDMN and rCEN in the BD and MDD patients. On the other side, we found the specific alteration of decreased dFNC variability between aDMN and rCEN in the MDD patients. Our findings suggested the decreased ability of information processing and communication in BD and MDD patients, which may help us to understand their abnormal affective and cognitive functions clinically.

References

Abbott AE, Nair A, Keown CL, Datko M, Jahedi A, Fishman I and Muller RA (2016) Patterns of atypical functional connectivity and behavioral links in autism differ between default, salience, and executive networks. *Cerebral Cortex* **26**, 4034–4045.

Allen EA, Damaraju E, Plis SM, Erhardt EB, Eichele T and Calhoun VD (2014) Tracking whole-brain connectivity dynamics in the resting state. *Cerebral Cortex* **24**, 663–676.

Angst J, Cui L, Swendsen J, Rothen S, Cravchik A, Kessler RC and Merikangas KR (2010) Major depressive disorder with subthreshold bipolarity in the national comorbidity survey replication. *American Journal of Psychiatry* **167**, 1194–1201.

Bai F, Shu N, Yuan YG, Shi YM, Yu H, Wu D, Wang JH, Xia MR, He Y and Zhang ZJ (2012) Topologically convergent and divergent structural connectivity patterns between patients with remitted geriatric depression and amnestic mild cognitive impairment. *Journal of Neuroscience* **32**, 4307–4318.

Barttfeld P, Uhrig L, Sitt JD, Sigman M, Jarraya B and Dehaene S (2015) Signature of consciousness in the dynamics of resting-state brain activity. *Proceedings of the National Academy of Sciences of the USA* **112**, 887–892.

Beckmann CF, DeLuca M, Devlin JT and Smith SM (2005) Investigations into resting-state connectivity using independent component analysis. *Philosophical Transactions of the Royal Society B-Biological Sciences* **360**, 1001–1013.

Bell AJ and Sejnowski TJ (1995) An information-maximization approach to blind separation and blind deconvolution. *Neural Computation* **7**, 1129–1159.

Broyd SJ, Demanuele C, Debener S, Helps SK, James CJ and Sonuga-Barke EJS (2009) Default-mode brain dysfunction in mental disorders: a systematic review. *Neuroscience and Biobehavioral Reviews* **33**, 279–296.

Calhoun V (2004) Group ICA of fMRI toolbox (GIFT). Available at http://icatb.sourceforge.net.

Calhoun V, Adali T, Pearlson G and Pekar J (2001) A method for making group inferences from functional MRI data using independent component analysis. *Human brain mapping* **14**, 140–151.

Chen AC, Oathes DJ, Chang C, Bradley T, Zhou ZW, Williams LM, Glover GH, Deisseroth K and Etkin A (2013) Causal interactions between fronto-parietal central executive and default-mode networks in humans. *Proceedings of the National Academy of Sciences of the USA* **110**, 19944–19949.

Chen L, Wang Y, Niu C, Zhong S, Hu H, Chen P, Zhang S, Chen G, Deng F, Lai S, Wang J, Huang L and Huang R (2018) Common and distinct abnormal frontal-limbic system structural and functional patterns in patients with major depression and bipolar disorder. *Neuroimage Clinical* **20**, 42–50.

Damoiseaux JS, Rombouts SA, Barkhof F, Scheltens P, Stam CJ, Smith SM and Beckmann CF (2006) Consistent resting-state networks across healthy subjects. *Proceedings of the National Academy of Sciences of the USA* **103**, 13848–13853.

de Almeida JRC and Phillips ML (2013) Distinguishing between unipolar depression and bipolar depression: current and future clinical and neuroimaging perspectives. *Biological Psychiatry* **73**, 111–118.

de Kwaasteniet BP, Rive MM, Ruhé HG, Schene AH, Veltman DJ, Fellinger L, van Wingen GA and Denys D (2014) Decreased resting-state connectivity between neurocognitive networks in treatment resistant depression. *Frontiers in psychiatry* **6**, 28–28.

Demirtas M, Tornador C, Falcon C, Lopez-Sola M, Hernandez-Ribas R, Pujol J, Menchon JM, Ritter P, Cardoner N, Soriano-Mas C and Deco G (2016) Dynamic functional connectivity reveals altered variability in functional connectivity among patients with major depressive disorder. *Human Brain Mapping* **37**, 2918–2930.

Diener C, Kuehner C, Brusniak W, Ubl B, Wessa M and Flor H (2012) A meta-analysis of neurofunctional imaging studies of emotion and cognition in major depression. *Neuroimage* **61**, 677–685.

Dong D, Ming Q, Zhong X, Pu W, Zhang X, Jiang Y, Gao Y, Sun X, Wang X and Yao S (2018) State-independent alterations of intrinsic brain network in current and remitted depression. *Progress in Neuropsychopharmacology & Biological Psychiatry* **89**, 475–480.

Fountoulakis KN (2010) The emerging modern face of mood disorders: a didactic editorial with a detailed presentation of data and definitions. *Annals of General Psychiatry* 9, 14.

Fox MD, Snyder AZ, Vincent JL, Corbetta M, Van Essen DC and Raichle ME (2005) The human brain is intrinsically organized into dynamic, anticorrelated functional networks. *Proceedings of the National Academy of Sciences of the USA* 102, 9673–9678.

Fransson P (2005) Spontaneous low-frequency BOLD signal fluctuations: an fMRI investigation of the resting-state default mode of brain function hypothesis. *Human Brain Mapping* 26, 15–29.

Gong Q, Hu X, Pettersson-Yeo W, Xu X, Lui S, Crossley N, Wu M, Zhu H and Mechelli A (2017) Network-level dysconnectivity in drug-naive first-episode psychosis: dissociating transdiagnostic and diagnosis-specific alterations. *Neuropsychopharmacology* 42, 933–940.

Gong J, Chen G, Jia Y, Zhong S, Zhao L, Luo X, Qiu S, Lai S, Qi Z, Huang L and Wang Y (2019) Disrupted functional connectivity within the default mode network and salience network in unmedicated bipolar II disorder. *Progress in Neuropsychopharmacology & Biological Psychiatry* 88, 11–18.

Gonzalez-Castillo J, Hoy CW, Handwerker DA, Robinson ME, Buchanan LC, Saad ZS and Bandettini PA (2015) Tracking ongoing cognition in individuals using brief, whole-brain functional connectivity patterns. *Proceedings of the National Academy of Sciences of the USA* 112, 8762–8767.

Goulden N, Khusnulina A, Davis NJ, Bracewell RM, Bokde AL, McNulty JP and Mullins PG (2014) The salience network is responsible for switching between the default mode network and the central executive network: replication from DCM. *Neuroimage* 99, 180–190.

Goya-Maldonado R, Brodmann K, Keil M, Trost S, Dechent P and Gruber O (2016) Differentiating unipolar and bipolar depression by alterations in large-scale brain networks. *Human Brain Mapping* 37, 808–818.

He Y, Wang Y, Chang TT, Jia Y, Wang J, Zhong S, Huang H, Sun Y, Deng F, Wu X, Niu C, Huang L, Ma G and Huang R (2018) Abnormal intrinsic cerebro-cerebellar functional connectivity in un-medicated patients with bipolar disorder and major depressive disorder. *Psychopharmacology* (Berl). doi: 10.1007/s00213-018-5021-6.

Himberg J, Hyvarinen A and Esposito F (2004) Validating the independent components of neuroimaging time series via clustering and visualization. *Neuroimage* 22, 1214–1222.

Hutchison RM and Morton JB (2015) Tracking the brain's functional coupling dynamics over development. *Journal of Neuroscience* 35, 6849–6859.

Jiang Y, Duan M, Chen X, Chang X, He H, Li Y, Luo C and Yao D (2017) Common and distinct dysfunctional patterns contribute to triple network model in schizophrenia and depression: a preliminary study. *Progress in Neuropsychopharmacology & Biological Psychiatry* 79, 302–310.

Kaiser RH, Whitfield-Gabrieli S, Dillon DG, Goer F, Beltzer M, Minkel J, Smoski M, Dichter G and Pizzagalli DA (2016) Dynamic resting-state functional connectivity in major depression. *Neuropsychopharmacology* 41, 1822–1830.

Karahanoglu FI and Van De Ville D (2015) Transient brain activity disentangles fMRI resting-state dynamics in terms of spatially and temporally overlapping networks. *Nature Communications* 6, 7751.

Leonardi N and Van De Ville D (2015) On spurious and real fluctuations of dynamic functional connectivity during rest. *Neuroimage* 104, 430–436.

Leow A, Ajilore O, Zhan L, Arienzo D, GadElkarim J, Zhang A, Moody T, Van Horn J, Feusner J, Kumar A, Thompson P and Altshuler L (2013) Impaired inter-hemispheric integration in bipolar disorder revealed with brain network analyses. *Biological Psychiatry* 73, 183–193.

Li X, Steffens DC, Potter GG, Guo H, Song S and Wang L (2017) Decreased between-hemisphere connectivity strength and network efficiency in geriatric depression. *Human Brain Mapping* 38, 53–67.

Maddock RJ (1999) The retrosplenial cortex and emotion: new insights from functional neuroimaging of the human brain. *Trends in Neurosciences* 22, 310–316.

Manoliu A, Riedl V, Doll A, Bauml JG, Muhlau M, Schwerthoffer D, Scherr M, Zimmer C, Forstl H, Bauml J, Wohlschlager AM, Koch K and Sorg C (2013) Insular dysfunction reflects altered between-network connectivity and severity of negative symptoms in schizophrenia during psychotic remission. *Frontiers in Human Neuroscience* 7, 216.

Manoliu A, Meng C, Brandl F, Doll A, Tahmasian M, Scherr M, Schwerthoffer D, Zimmer C, Forstl H, Bauml J, Riedl V, Wohlschlager AM and Sorg C (2014a) Insular dysfunction within the salience network is associated with severity of symptoms and aberrant inter-network connectivity in major depressive disorder. *Frontiers in Human Neuroscience* 7, 930.

Manoliu A, Riedl V, Zherdin A, Muhlau M, Schwerthoffer D, Scherr M, Peters H, Zimmer C, Forstl H, Bauml J, Wohlschlager AM and Sorg C (2014b) Aberrant dependence of default mode/central executive network interactions on anterior insular salience network activity in schizophrenia. *Schizophrenia Bulletin* 40, 428–437.

Marusak HA, Calhoun VD, Brown S, Crespo LM, Sala-Hamrick K, Gotlib IH and Thomason ME (2017) Dynamic functional connectivity of neurocognitive networks in children. *Human Brain Mapping* 38, 97–108.

McGuffin P, Rijsdijk F, Andrew M, Sham P, Katz R and Cardno A (2003) The heritability of bipolar affective disorder and the genetic relationship to unipolar depression. *Archives of General Psychiatry* 60, 497–502.

Meda SA, Ruano G, Windemuth A, O'Neil K, Berwise C, Dunn SM, Boccaccio LE, Narayanan B, Kocherla M, Sprooten E, Keshavan MS, Tamminga CA, Sweeney JA, Clementz BA, Calhoun VD and Pearlson GD (2014) Multivariate analysis reveals genetic associations of the resting default mode network in psychotic bipolar disorder and schizophrenia. *Proceedings of the National Academy of Sciences of the USA* 111, E2066–E2075.

Meng C, Brandl F, Tahmasian M, Shao JM, Manoliu A, Scherr M, Schwerthoffer D, Bauml J, Forstl H, Zimmer C, Wohlschlager AM, Riedl V and Sorg C (2014) Aberrant topology of striatum's connectivity is associated with the number of episodes in depression. *Brain* 137, 598–609.

Menon V (2011) Large-scale brain networks and psychopathology: a unifying triple network model. *Trends in Cognitive Sciences* 15, 483–506.

Murphy K, Birn RM, Handwerker DA, Jones TB and Bandettini PA (2009) The impact of global signal regression on resting state correlations: are anti-correlated networks introduced? *Neuroimage* 44, 893–905.

Negwer C, Beurskens E, Sollmann N, Maurer S, Ille S, Giglhuber K, Kirschke JS, Ringel F, Meyer B and Krieg SM (2018) Loss of subcortical language pathways correlates with surgery-related aphasia in patients with brain tumor: an investigation via repetitive navigated transcranial magnetic stimulation-based diffusion tensor imaging fiber tracking. *World Neurosurgery* 111, e806–e818.

Nguyen TT, Kovacevic S, Dev SI, Lu K, Liu TT and Eyler LT (2017) Dynamic functional connectivity in bipolar disorder is associated with executive function and processing speed: a preliminary study. *Neuropsychology* 31, 73–83.

Niu M, Wang Y, Jia Y, Wang J, Zhong S, Lin J, Sun Y, Zhao L, Liu X, Huang L and Huang R (2017) Common and specific abnormalities in cortical thickness in patients with Major depressive and bipolar disorders. *EBioMedicine* 16, 162–171.

Pang Y, Chen H, Wang Y, Long Z, He Z, Zhang H, Liao W, Cui Q and Chen H (2018) Transdiagnostic and diagnosis-specific dynamic functional connectivity anchored in the right anterior insula in major depressive disorder and bipolar depression. *Progress in Neuropsychopharmacology & Biological Psychiatry* 85, 7–15.

Raichle ME, MacLeod AM, Snyder AZ, Powers WJ, Gusnard DA and Shulman GL (2001) A default mode of brain function. *Proceedings of the National Academy of Sciences of the USA* 98, 676–682.

Rashid B, Damaraju E, Pearlson GD and Calhoun VD (2014) Dynamic connectivity states estimated from resting fMRI identify differences among schizophrenia, bipolar disorder, and healthy control subjects. *Frontiers in Human Neuroscience* 8, 897.

Rashid B, Arbabshirani MR, Damaraju E, Cetin MS, Miller R, Pearlson GD and Calhoun VD (2016) Classification of schizophrenia and bipolar patients using static and dynamic resting-state fMRI brain connectivity. *Neuroimage* 134, 645–657.

Shanahan M (2010) Metastable chimera states in community-structured oscillator networks. *Chaos* 20, 013108.

Sheline YI, Price JL, Yan ZZ and Mintun MA (2010) Resting-state functional MRI in depression unmasks increased connectivity between networks via the dorsal nexus. *Proceedings of the National Academy of Sciences of the USA* **107**, 11020–11025.

Smith SM, Fox PT, Miller KL, Glahn DC, Fox PM, Mackay CE, Filippini N, Watkins KE, Toro R, Laird AR and Beckmann CF (2009) Correspondence of the brain's functional architecture during activation and rest. *Proceedings of the National Academy of Sciences of the USA* **106**, 13040–13045.

Sridharan D, Levitin DJ and Menon V (2008) A critical role for the right fronto-insular cortex in switching between central-executive and default-mode networks. *Proceedings of the National Academy of Sciences of the USA* **105**, 12569–12574.

Tagliazucchi E and Laufs H (2014) Decoding wakefulness levels from typical fMRI resting-state data reveals reliable drifts between wakefulness and sleep. *Neuron* **82**, 695–708.

Tognoli E and Kelso JA (2014) The metastable brain. *Neuron* **81**, 35–48.

Vandeleur CL, Merikangas KR, Strippoli MP, Castelao E and Preisig M (2014) Specificity of psychosis, mania and major depression in a contemporary family study. *Molecular Psychiatry* **19**, 209–213.

Wang Y, Zhong S, Jia Y, Zhou Z, Wang B, Pan J and Huang L (2015) Interhemispheric resting state functional connectivity abnormalities in unipolar depression and bipolar depression. *Bipolar Disorder* **17**, 486–495.

Wang L, Shen H, Lei Y, Zeng LL, Cao F, Su L, Yang Z, Yao S and Hu D (2017*a*) Altered default mode, fronto-parietal and salience networks in adolescents with Internet addiction. *Addictive Behaviors* **70**, 1–6.

Wang Y, Wang J, Jia Y, Zhong S, Niu M, Sun Y, Qi Z, Zhao L, Huang L and Huang R (2017*b*) Shared and specific intrinsic functional connectivity patterns in unmedicated bipolar disorder and Major depressive disorder. *Scientific Reports* **7**, 3570.

Wang Y, Wang J, Jia Y, Zhong S, Zhong M, Sun Y, Niu M, Zhao L, Zhao L, Pan J, Huang L and Huang R (2017*c*) Topologically convergent and divergent functional connectivity patterns in unmedicated unipolar depression and bipolar disorder. *Translational Psychiatry* **7**, e1165.

Wang J, Wang Y, Wu X, Huang H, Jia Y, Zhong S, Wu X, Zhao L, He Y, Huang L and Huang R (2018) Shared and specific functional connectivity alterations in unmedicated bipolar and major depressive disorders based on the triple-network model. *Brain Imaging and Behavior*. doi: 10.1007/s11682-018-9978-x.

Wei M, Qin J, Yan R, Bi K, Liu C, Yao Z and Lu Q (2015) Association of resting-state network dysfunction with their dynamics of inter-network interactions in depression. *Journal of Affective Disorder* **174**, 527–534.

Wise T, Marwood L, Perkins AM, Herane-Vives A, Joules R, Lythgoe DJ, Luh WM, Williams SCR, Young AH, Cleare AJ and Arnone D (2017) Instability of default mode network connectivity in major depression: a two-sample confirmation study. *Translational Psychiatry* **7**, e1105.

Ye T, Peng J, Nie B, Gao J, Liu J, Li Y, Wang G, Ma X, Li K and Shan B (2012) Altered functional connectivity of the dorsolateral prefrontal cortex in first-episode patients with major depressive disorder. *European Journal of Radiology* **81**, 4035–4040.

Young RC, Biggs JT, Ziegler VE and Meyer DA (1978) A rating scale for mania: reliability, validity and sensitivity. *British Journal of Psychiatry* **133**, 429–435.

Zhao L, Wang Y, Jia Y, Zhong S, Sun Y, Qi Z, Zhang Z and Huang L (2017) Altered interhemispheric functional connectivity in remitted bipolar disorder: a resting state fMRI study. *Scientific Reports* **7**, 4698.

Zheng H, Xu L, Xie F, Guo X, Zhang J, Yao L and Wu X (2015) The altered triple networks interaction in depression under resting state based on graph theory. *Biomed Research International* **2015**, 386326.